

NONLINEAR DYNAMICS STUDIES AT THE CERN PROTON SYNCHROTRON: PRECISE MEASUREMENTS OF ISLANDS PARAMETERS FOR THE NOVEL MULTI-TURN EXTRACTION

M. Giovannozzi, P. Scaramuzzi, CERN, Geneva, Switzerland

Abstract

Recently, a novel approach to perform multi-turn extraction from a circular accelerator was proposed. It is based on adiabatic capture of particles into islands of transverse phase space generated by nonlinear resonances. Sextupole and octupole magnets are used to generate these islands, while an appropriate slow variation of the linear tune allows particles to be trapped inside the islands. Intense experimental efforts showed that the approach is indeed performing rather well. However, good knowledge of the islands properties is a key ingredient for the success of this extraction type. In this paper, a series of measurements are presented dealing with the study of islands' parameters for the fourth-order resonance, such as detuning with amplitude, fixed points' position, betatron frequency inside the islands.

INTRODUCTION

Since the approval of the CERN Neutrino to Gran Sasso Project (CNGS) [1] the special extraction mode, the so-called Continuous Transfer (CT) [2], was reviewed in detail to propose an improved scheme for beam extraction from the CERN Proton Synchrotron (PS) to the Super Proton Synchrotron (SPS).

Recently, an alternative method was proposed, where the beam is split in the transverse phase space by means of adiabatic capture inside stable islands of the fourth-order resonance [3]. Intense efforts were devoted to its experimental demonstration since the year 2002 [4] and these studies were pursued during the whole 2003 run [5, 6].

The knowledge of the islands' parameters, such as position and size, is of paramount importance for the novel approach. The stable islands are generated by means of sextupoles and octupoles installed in PS section 21 and 20, respectively. The information concerning the phase space is based on turn-by-turn acquisition of the beam trajectory by means of two pickups 90° apart [4, 7] and the standard choice consists in selecting those in sections 63 and 67. The beam trajectory is perturbed by the kicker magnet normally used to fast extract the beam. To avoid as much as possible beam filamentation effects a single-bunch, low-intensity, pencil beam is used, featuring an intensity of 40×10^{10} protons, normalised rms emittances of $1.7 \mu\text{m}$ and $1.55 \mu\text{m}$ in the horizontal and vertical plane, respectively. The relative rms momentum spread is 0.25×10^{-3} at 14 GeV/c.

A sketch of the PS circumference together with the key elements used in the experiments is shown in Fig. 1.

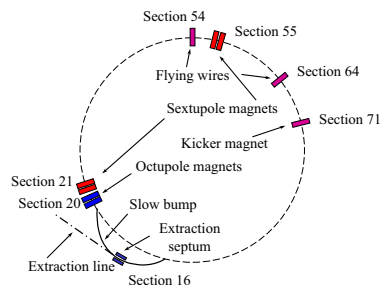


Figure 1: Layout of the PS machine including the key elements used for the measurements of islands properties.

THEORETICAL BACKGROUND

The one-turn map \mathcal{M} of the PS machine is analysed using the normal forms approach [8]. Assuming that a 2D version of the measured PS lattice [9] is used, including a sextupolar and an octupolar element, represented in the single-kick approximation [8], located in sections 21 and 20, respectively, the beam dynamics in the neighbourhood of the fourth-order resonance is described by the following hamiltonian [8, 10]

$$\mathcal{H}(\rho, \theta) = \epsilon\rho + \frac{\rho^2 \Omega_2}{2} + \epsilon\rho^2 |u_{0,3}| \cos(4\theta + \psi), \quad (1)$$

where (ρ, θ) are action-angle coordinates in the normal form space and the quantities $\epsilon, \Omega_2, u_{0,3}$ are defined as

$$\begin{aligned} \epsilon &= \omega - \frac{\pi}{2} \\ \Omega_2 &= -\frac{1}{16} \left[3 \cot\left(\frac{\omega}{2}\right) + \cot\left(\frac{3\omega}{2}\right) \right] - \frac{3}{8}\kappa \end{aligned} \quad (2)$$

$$\begin{aligned} 8u_{0,3} &= -i\kappa \cos(\omega) + i e^{i(\omega-4\Delta\psi)} \cos\left(\frac{\omega}{2}\right) \csc\left(\frac{3\omega}{2}\right) \\ &\quad + \kappa \sin(\omega), \end{aligned}$$

while κ is given by

$$\kappa = \frac{2}{3} \frac{K_3 \beta_{\text{Oct}}^2}{K_2^2 \beta_{\text{Sex}}^3} \quad \text{with} \quad K_m = \frac{1}{B\rho} \frac{d^m B_y}{dx^m}. \quad (3)$$

In the previous equations, $\beta_{\text{Sex,Oct}}$ stands for the value of the horizontal beta-function at the sextupole and octupole location, respectively; $\Delta\psi$ represents the horizontal betatron phase advance between them; $B\rho$ is the magnetic rigidity, and B_y is the vertical component of the magnetic field in the considered element. The physical meaning of the various quantities is clear: Ω_2 represents the detuning with amplitude and $u_{0,3}$ the first resonant term, responsible for the islands' generation. From Eq. (1) the expression of islands properties such as the fixed point position (islands centre) ρ_+ , the island surface Σ , and the secondary

frequency ω_{sec} , i.e. the central frequency of the pendulum-like hamiltonian (1) can be easily derived

$$\rho_+ = -\frac{\epsilon}{\Omega_2 + 2\epsilon|u_{0,3}|} \quad \omega_{\text{sec}} = 4\sqrt{|\epsilon u_{0,3}\Omega_2\rho_+^2|}$$

$$\Sigma = 16\sqrt{\left|\frac{\epsilon u_{0,3}\rho_+^2}{\Omega_2}\right|}. \quad (4)$$

Interestingly enough, it is possible to link directly the islands' surface and two quantities directly observable, such as Ω_2 and ω_{sec}

$$\Sigma = 4\frac{\omega_{\text{sec}}}{|\Omega_2|} \quad (5)$$

EXPERIMENTAL RESULTS

The experimental data have been analysed to derive beam frequency, around the origin and inside the islands, using the techniques presented in Ref. [11], in particular, applying the Hanning filter to measured data [11]. The error associated with this method scales as N^{-4} , N being the number of turns, provided the beam position is not affected by noise, otherwise it scales as N^{-2} [11]. In the analysis presented here the value $2/N^2$ has been assumed. As far as the accuracy of the pickups is concerned, the electronic noise was measured to be of the order of 0.2 mm rms, while the absolute precision is believed to be about 1 mm, which is the value assumed in the error analysis presented here. An example of phase space measurement with a clear signature of stable islands is shown in Fig. 2. The four spots

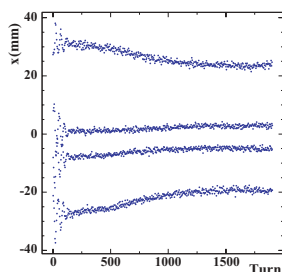


Figure 2: Measured horizontal beam position vs. time for the pickup in section 63.

represent the islands' position, while beam position oscillations right after the kick reveal that the beam is rotating around the island's centre. Then, filamentation occurs until such oscillations are completely damped. The slow variation over time of the islands' position is very likely due to particles' diffusion outside the islands induced by longitudinal motion. It is worthwhile stressing that under the influence of nonlinear forces the beam filamentation might lead to a non-zero asymptotic signal [12]. In fact, the distortion induced by transverse nonlinearities, the so-called smear, i.e. the relative standard deviation of the linear invariant over the orbit, might break the perfect central symmetry of the orbit, thus resulting in a non-zero signal on a beam position monitor. Of course, a non-zero value of the centre-of-gravity of the charge distribution implies a non-zero smear, but the converse is not true.

Detuning with Amplitude

This is a rather standard measurement. The maximum beam amplitude has to be smaller than the islands' position, in order to sample only the phase space where regular motion occurs. In Fig. 3 the experimental data are plotted together with the results of numerical simulations based on the 2D model of the PS machine. Only 128 measured turns have been used for tune computation to avoid the signal damping due to filamentation. Also, a convex hull algorithm allowed determining the border of the phase space region occupied by the beam and then to compute its area as an estimate of the invariant of motion. The agreement be-

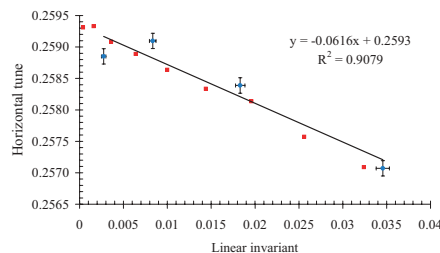


Figure 3: Horizontal tune vs. the linear invariant in the normal form space for both experimental and simulation data. The straight line is a fit of the experimental data.

tween experimental and simulation data is very good. The straight line represents the fit of the experimental data and is in excellent agreement with numerical simulation results.

Position of Fixed Points

By increasing its amplitude, the beam samples the fraction of phase space where stable islands of the fourth-order resonance are located. Typical results are shown in Fig. 4 where the phase space for an initial condition inside the islands is shown for about 2000 turns (upper). The apparent amplitude reduction is due to beam filamentation. This effect disappears when the first 15 turns are plotted (lower part of Fig. 4). The orbits are closing inside each island, thus allowing the computation of an average position (shown as a cross in the figure) to be compared with the theoretical position ρ_+ (open square) of the fixed point (after transforming back to the physical coordinates). An excellent agreement is found between ρ_+ and the average over the beam position for all the islands but the one in the first quadrant, for which the theoretical position of the fixed point falls outside the measured orbit. Investigations to understand this feature are in progress. The good agreement found for the other three islands seems to indicate that the orbits are only slightly deformed with respect to a circle, thus making the average value over one complete revolution about the fixed point a good approximation of the actual fixed point position.

Secondary Frequency

Indeed, from the turn-by-turn measurements inside the islands one can extract much more information than the

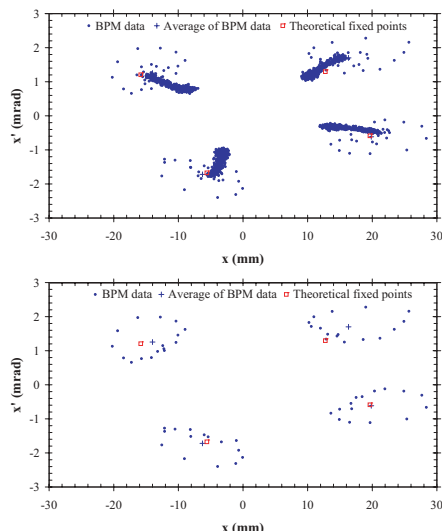


Figure 4: Measured horizontal phase space (upper). A detail of the first 15 turns is also shown (lower). The theoretical fixed points' position is shown, together with the average position over the first 15 turns.

simple fixed point location. In fact, the first few turns can be used to compute the so-called secondary frequency, i.e. the betatron frequency around the fixed point. An analytical estimate is also available, by computing the zero-amplitude frequency for the pendulum-like hamiltonian (1). To remove the strong component originating from the fourth-order resonance from the measure spectrum, a stroboscopic analysis was applied, taking only each fourth point in the time-series. The frequency analysis is then performed in exactly the same way as for the detuning with amplitude measurement: in this case only 64 turns have been considered as the oscillations are strongly damped (see Fig. 2). The time-series corresponding to 19 different initial amplitudes in the islands' region yield the average value $\omega_{\text{sec}}^{\text{meas}} = (0.0375 \pm 0.0008)$, which is in excellent agreement with the theoretical value $\omega_{\text{sec}}^{\text{th}} = 0.039$ [10].

A refined analysis was also attempted. In fact, as the kicker strength is different for each time-series, the variation of ω_{sec} as a function of the distance from the fixed point could be extracted from measured data. In analogy with what was done for the detuning with amplitude, the secondary frequency has been computed as a function of the area of the orbit inside each island, assuming that this should be an approximate invariant of motion. These data have been compared with numerical simulations and the outcome is plotted in Fig. 5. The good agreement is clearly visible, in spite of the measurement errors (probably underestimated). The straight lines represent the linear fit to the data. In the case of the experimental points, a weighted fit has been applied, yielding $\omega_{\text{sec}}^{\text{meas}} = (0.0408 \pm 0.0009)$, which is even closer to the theoretical result.

CONCLUSIONS AND OUTLOOK

A series of measurements of nonlinear beam dynamics were performed in the framework of the studies for the

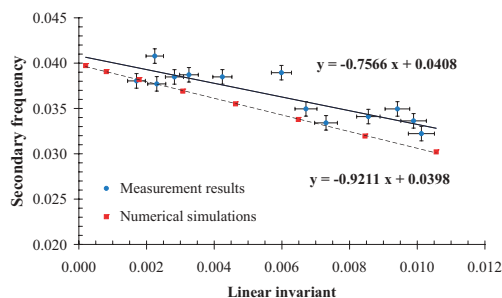


Figure 5: Secondary frequency ω_{sec} vs. the surface, in the normal form space, covered by the orbit inside the island for both experimental and simulation data.

novel extraction based on adiabatic capture inside stable islands of transverse phase space. Detuning with amplitude, fixed points' position, secondary frequency inside the islands have been measured and compared with both theoretical computations and results of numerical simulations, showing a very good agreement. This increases our confidence in the theoretical predictions based on the model (1). The next step will consist in using the theoretical tools developed so far, i.e. the knowledge about islands' properties, to improve the extracted beam parameters as well as guiding the beam manipulations during the adiabatic capture process. [10].

REFERENCES

- [1] K. Elsener (Ed.) *et al.*, *CERN 98-02* (1998).
- [2] C. Bovet, D. Fiander, L. Henny, A. Krusche, G. Plass, in *1973 Particle Accelerator Conference*, edited by D. W. Dupen (IEEE, New York), 1973, p. 438.
- [3] R. Capi, M. Giovannozzi, *Phys. Rev. Lett.* **88**, 104801, (2002).
- [4] R. Capi, M. Giovannozzi, M. Martini, E. Métral, A.-S. Müller, and R. Steerenberg, in *PAC2003 Conference*, edited by J. Chew, P. Lucas and S. Webber (IEEE Computer Society Press, Piscataway), 2003, p. 388.
- [5] M. Giovannozzi (Ed.) *et al.*, *CERN-AB-2004-003-ABP* (2004).
- [6] M. Giovannozzi, R. Capi, S. Gilardoni, M. Martini, E. Métral, A. Sakumi, R. Steerenberg, A.-S. Müller, these proceedings.
- [7] M. E. Angoletta, M. Giovannozzi, M. Martini, E. Métral, G. Métral, A.-S. Müller, R. Steerenberg, in *Eighth Particle European Accelerator Conference*, edited by J. Poole and C. Petit-Jean-Genaz (Institute of Physics, UK London), 2002, p. 1273.
- [8] A. Bazzani, E. Todesco, G. Turchetti, and G. Servizi, *CERN 1994-02* (1994).
- [9] R. Capi, M. Giovannozzi, M. Martini, E. Métral, A.-S. Müller, and R. Steerenberg, in *PAC2003 Conference*, edited by J. Chew, P. Lucas and S. Webber (IEEE Computer Society Press, Piscataway), 2003, p. 2913.
- [10] M. Giovannozzi, P. Scaramuzzi, in preparation.
- [11] R. Bartolini, A. Bazzani, M. Giovannozzi, W. Scandale and E. Todesco, *Part. Accel.* **52**, 147, (1995).
- [12] A.-S. Müller, *CERN-PS (AE) 2002-007* (2002).